Comparison of Indirect and Stimulated Echo Compensated T2 Relaxometry Techniques: Extended Phase Graph vs Shinnar-Le Roux Based Modelling

Kelly C McPhee[1] and Alan H Wilman[2]

[1]*Physics, University of Alberta, Edmonton, Alberta, Canada,* [2]*Biomedical Engineering, University of Alberta, Edmonton, Alberta, Canada*

INTRODUCTION: Recent works have implemented means to fit for single component T_2 from multi-echo spin echo experiments with indirect and stimulated echo compensation [1,2,3]. These works used either the extended phase graph [1] or Shinnar Le Roux and Bloch simulations [2,3] to model complete echo pathways. We have recently demonstrated [2] T_2 fitting which makes use of prior knowledge of the flip angles and full simulations of the pulse sequence, instead of the Fourier approximation of slice profiles implemented by Lebel [1]. However, this approach has yet to be compared to the EPG-ISEC standard [1]. Here, we compare these two methods of indirect and stimulated echo compensation (ISEC) using both simulations and human brain MRI data.

METHODS:

Human brain imaging experiments were performed at 4.7 T in eight healthy volunteers (aged 30±5). Multi-echo spin echo (MESE) images were acquired through iron-rich deep grey matter (TR = 3 s; ETL = 32; TE = 10 to 320 ms; echo spacing = 10 ms; prescribed excitation = 90°; refocusing = 180°; relative refocusing width = 1.75; matrix = 256 x 145; voxel size = 1 x 1.25 x 4 mm^3).

Flip angle (FA) maps were acquired using the double angle method [4] with a correction for slice profile (geometry and pulse shapes matched to multi-echo data, TR = 7 s; FA = 60°, 120°; effective TE = 43 ms). Normalized FA maps (B_1) are expressed as a ratio of the FA achieved at the centre of the slice relative to the requested FA.

T_2 fitting was performed using the original ISEC [1], or fully simulated MESE sequences [2] to compensate for both spin echo and stimulated echo pathways. Lebel's method makes use of Fourier slice profiles, and the extended phase graph [5] algorithm to simulate sequences and fit for both T_2 and flip angle. In our implementation, slice selective RF pulses were simulated using the Shinnar-Le Roux algorithm [6], and relaxation between pulses was calculated according to Bloch equation solutions. T_1 is assumed to be 3 s to calculate the fit curves. T_2 maps were computed with both methods. The FA map was provided to the Bloch-ISEC fitting algorithm.

Simulation Experiments were performed to examine T_2 fitting accuracy, and efficacy over a range of relative refocussing widths. Both ISEC methods were used to fit fully simulated multi-echo spin echo curves (T_2 = 10-140 ms, B_1 = 0.5-1.5, T_1 = 1 s), with parameters matched to experimental data (pulse shapes, gradients, timing). Fitting was also performed for select T_2 values (30 ms, 50 ms, and 75 ms) at a range of relative refocussing widths (1-4) and B_1 values (0.5-1.5). Simulations of decay curves, and all image processing were performed in MATLAB using custom in-house code.

RESULTS:

T_2 fitting accuracy as a function of T_2 and normalized flip angle map (B_1) value is shown in Fig 1 for (a) Bloch-ISEC and (b) EPG-ISEC. Accuracy is improved using the Bloch simulation based method, particularly at low T_2 values. Fit accuracy at a range of relative refocussing widths is examined in Fig 2. Bloch-ISEC outperforms EPG-ISEC in all cases, but most notably at short T_2 values, even at relatively wide refocussing widths. In Fig 3, example T_2 maps (a-b) and corresponding B_1 maps (d-e), from one subject are shown. Table 1 shows T_2 values from various grey and white matter regions, averaged over six healthy volunteers. Differences in *in vivo* results between the two methods agree with theoretical differences in the models.

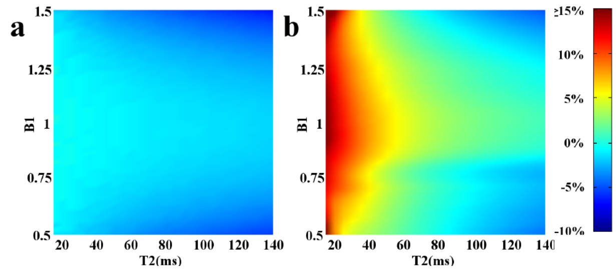

Figure 1: *T_2 fitting accuracy is examined for a range of T_2 and B_1 values using (a) Bloch-ISEC and (b) EPG-ISEC.*

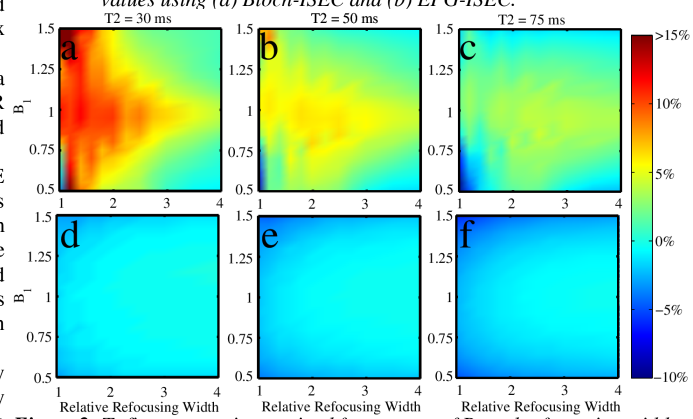

Figure 2: *T_2 fit accuracy is examined for a range of B_1 and refocussing widths using (a-c) EPG-ISEC and (d-f) Bloch-ISEC where (a,d) T_2 = 30 ms, (b,e) 50 ms, and (c,f) 75 ms.*

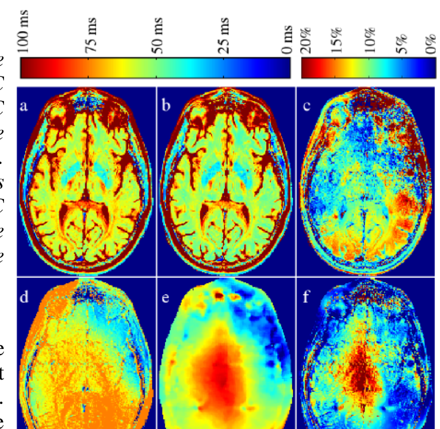

Figure 3: *T_2 maps (ms) are shown from (a) EPG-ISEC fitting, (b) Bloch-ISEC fitting, and the difference (c) |a-b| (%). Corresponding B_1 maps using (d) fit with EPG-ISEC and (e) double angle method, and the difference (f) e-d.*

DISCUSSION:

Due to the fundamental difference in modelling of selective RF pulses between the two fitting models, the limitations of each approach are distinct and different. However these different ISEC fitting approaches have not previously been compared in literature. The Bloch approach discussed here requires accurate knowledge of the FA. Others have implemented a dual T_2 and FA Bloch approach [6], but it has also not been compared to EPG-ISEC. The EPG method also fits for both T_2 and FA and the resulting underestimated FA (Fig 3d) is compensated for by overestimating magnetization width and inflating the contribution of stimulated echoes [1] to still produce good accuracy in T_2. Thus EPG-ISEC is most effective without knowledge of FA. EPG-ISEC requires the assumption that refocussing angles are ≤180°, which is not always true [7]. Both Bloch-ISEC and EPG-ISEC algorithms have non-unique solutions with refocussing angles above and below 180°, and different T_2 values, when RF pulses are slice selective. Here we compared the original EPG based ISEC method to a Bloch-based method with independent flip angle measurement to avoid T_2 fitting errors which may arise from freely fitting for both parameters over a full range of refocussing angles. This step is potentially unnecessary if refocussing angles were purposefully prescribed to lower values, such that the fitting range may be limited, avoiding multiple solutions. In cases where the B_1 field is more uniform (such as at 1.5 T) and well known such that fitting parameters may be restricted, this step may also be avoided.

Table 1: Group averaged T_2 values from various grey matter and white matter regions[a]

Region	Mean T_2 (ms)		B_1	$T_{2,Bloch}$ - $T_{2,EPG}$ (ms)		N[b]
	EPG-ISEC	Bloch-ISEC		Measured	Theory	
Globus Pallidus	37.1 ± 1.8	33.8 ± 1.7	1.13 ± 0.15	-3.3 ± 0.8	-3.1 ± 0.2	7
Caudate Head	59.8 ± 2.4	56.6 ± 2.2	1.06 ± 0.13	-3.2 ± 1.1	-3.4 ± 0.3	8
Putamen	52.3 ± 3.1	49.0 ± 3.8	1.07 ± 0.16	-3.3 ± 1.4	-3.3 ± 0.3	8
Thalamus	55.6 ± 2.6	51.7 ± 2.0	1.13 ± 0.11	-3.9 ± 1.0	-3.3 ± 0.2	6
Posterior White Matter	64.5 ± 2.9	59.0 ± 3.0	1.01 ± 0.13	-5.5 ± 1.3	-3.4 ± 0.3	8
Frontal White matter	52.8 ± 1.6	50.1 ± 2.6	0.97 ± 0.11	-2.7 ± 1.7	-3.3 ± 0.3	7
Insular Cortex	73.7 ± 3.2	69.7 ± 3.7	1.03 ± 0.13	-3.9 ± 1.8	-3.3 ± 0.4	8
Cortical Grey Matter	60.5 ± 3.4	55.8 ± 3.7	0.93 ± 0.09	-4.7 ± 1.9	-3.3 ± 0.4	8

[a] Errors are reported as standard deviation within the group.
[b] N indicates the number of subjects used for each region. ROIs with inadequate SNR or B_1^+ values that were too low were rejected.

CONCLUSIONS:

By fully accounting for flip angle and slice selection, the Bloch-ISEC method enables accurate T_2 quantification over a wide range of refocussing angles, with improved accuracy over the EPG-ISEC method, particularly for T_2<50 ms.

REFERENCES: **[1]** Lebel RM, Wilman AH. MRM. 2010;64(4):1005-14. **[2]** McPhee KC, Wilman AH. Proc ISMRM-ESMRMB 2014. p. 3195. **[3]** Ben-Eliezer N, Sodickson DK, Block KT. MRM. 2014 Apr. **[4]** Stollberger R, Wach P. Magn Reson Med. 1996;35:246-51. **[5]** Hennig J. 1991;3(3):125-43. **[6]** Pauly J, Le Roux, P, Nishimura, D, Macovski, A. IEEE Trans Med Imag, 10(1):53-65, 1991. **[7]** Breitkreutz D, McPhee KC, Wilman AH. Proc ISMRM 21. 2013. p. 2466.